Electronic Supplementary Material (ESI) for Physical Chemistry Chemical Physics.

Supplemental Materials for

Disparate strain response of the thermal transport properties of bilayer penta-graphene as compared to that of monolayer penta-graphene

Zhehao Sun,[a] Kunpeng Yuan,[a] Xiaoliang Zhang*[a], Guangzhao Qin*[b], Xiaojing Gong*[c] and Dawei Tang*[a]

[a]*Key Laboratory of Ocean Energy Utilization and Energy Conservation of Ministry of Education, School of Energy and Power Engineering, Dalian University of Technology, Dalian 116024, China.*

[b]*Department of Mechanical Engineering, University of South Carolina, Columbia, SC 29208, USA.*

[c]*School of Materials Science & Engineering, Changzhou University, Changzhou 213164, China.*

Corresponding author. Email: zhangxiaoliang@dlut.edu.cn, qin.phys@gmail.com, gongxiaojing2018@cczu.edu.cn and dwtang@dlut.edu.cn

1. The convergence test of the thermal conductivity of monolayer and bilayer PG.

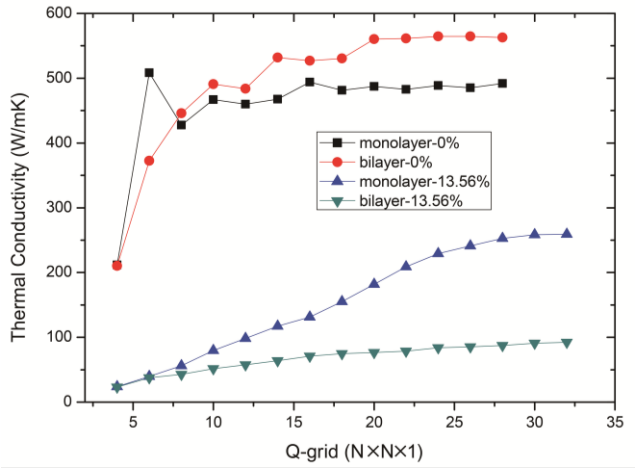

Fig. S1 The convergence test of thermal conductivity under no and high strain with the Q-grid of the Brillouin zone for the case of infinite size (L=100 μm) mono/bilayer PG.

We find that the thermal conductivity of both monolayer and bilayer PG are well convergent with a 28×28×1 Q-grid. Besides, due to the tremendous computing workload (primitive cell of bilayer PG having 12 atoms; the cutoff interactions up to the 12th nearest neighbors; considering vdW interactions), a 28×28×1 Q-grid for bilayer PG is a large value that can be considered.

2. Boltzmann transport equation (BTE)

The lattice thermal conductivity (κ) is calculated by iteratively solving the linearized Boltzmann transport equation (BTE) for phonons[1] as implemented in ShengBTE.[2]

At thermal equilibrium, the phonons are obeying Bose−Einstein distribution n_0. In the steady state with a temperature gradient ∇T generated, the new phonon distribution deviating from n_0 can be obtained from the BTE:

$$\frac{\partial n}{\partial t} = \nabla T \cdot \upsilon_{q\nu} \frac{\partial n}{\partial T}, \tag{1}$$

where n is the nonequilibrium distribution statistics, $q\nu$ means the phonon mode with a wave vector q and a polarization (branch) ν ($q\nu$ can be shortened as λ ($\lambda \equiv (q, \nu)$), $\upsilon_{q\nu}$ is the phonon group velocity which can be obtained by $\upsilon_{q\nu} = \partial\omega_{q\nu} / \partial q$, $\omega_{q\nu}$ is the phonon frequency. When ∇T is assumed small enough, Eq. (1) can be linearized and re-written as:[3]

$$n - n_0 = -F_{q\nu} \cdot \nabla T \frac{dn_0}{dT}, \tag{2}$$

where $F_{q\nu} = \tau_{q\nu}(\upsilon_{q\nu} + \Delta_{q\nu})$, which only considers three-phonon processes here,[4, 5] can be solved iteratively starting with a zeroth-order approximation.[2] Here, $\Delta_{q\nu}$ is used as a correction term of deviation to the relaxation time approximation (RTA)[6] results. $\tau_{q\nu}$ is the phonon relaxation time (phonon lifetime). The $\tau_{q\nu}$ can be computed by perturbation theory:[4, 5, 7]

$$\frac{1}{\tau_{q\nu}} = \frac{1}{N}\left(\sum_{\lambda\lambda'}^{+} \Gamma^{+}_{\lambda\lambda'\lambda''} + \sum_{\lambda\lambda'}^{-} \frac{1}{2}\Gamma^{-}_{\lambda\lambda'\lambda''} + \sum_{\lambda'} \Gamma_{\lambda\lambda'}\right), \tag{3}$$

where N is the number of discrete q sampling in the BZ, $\Gamma^{+}_{\lambda\lambda'\lambda''}$ and $\Gamma^{-}_{\lambda\lambda'\lambda''}$ respectively are three-phonon scattering rates of the absorption and emission processes, and $\Gamma_{\lambda\lambda'}$ is the scattering possibility from the disorder of isotopic impurity.[8] Based on the above

solution, the $\kappa_L^{\alpha\beta}$ can be obtained.

3. Effect of van der Waals (vdW) interaction

The influence of functionals of vdW on thermal properties has not received enough attention. In this section we will discuss the effect of vdW interaction on thermal properties of PG.

Table S1 Effect of exchange-correlation functionals on the thermal properties at 300K of heat capacity, thermal conductivity, frequency of ZA2 at Γ, phase space, average group velocity and the representative mean free path (rMFP).

	Monolayer No-vdW	Monolayer DFT-D	Bilayer No-vdW	Bilayer DFT-D	Bilayer vdW-DF2
Heat capacity (kJ/ m^{-3} /K)	1717	1722	1733	1939	1885
Thermal conductivity (W/mK)	491.4	518.2	591.3	562.8	590.5
Frequency of ZA2 at Γ (THz)	-	-	0.672	2.643	2.134
Phase space 10^{-8}	9.692	9.686	4.820	4.700	4.880
Average group velocity (m/s)	1828	1840	1805	1761	1729
rMFP (nm)	4171	4019	4303	3090	3109

Among all the implementations of vdW interactions, DFT-D[9, 10] and vdW-DF2[11-14] are two typical representative exchange-correlation functionals of vdW interactions, and we can gain a helpful estimation on the effect of vdW interactions on thermal properties of PG. The effects of exchange-correlation functionals on thermal properties of PG are shown in Table S1.

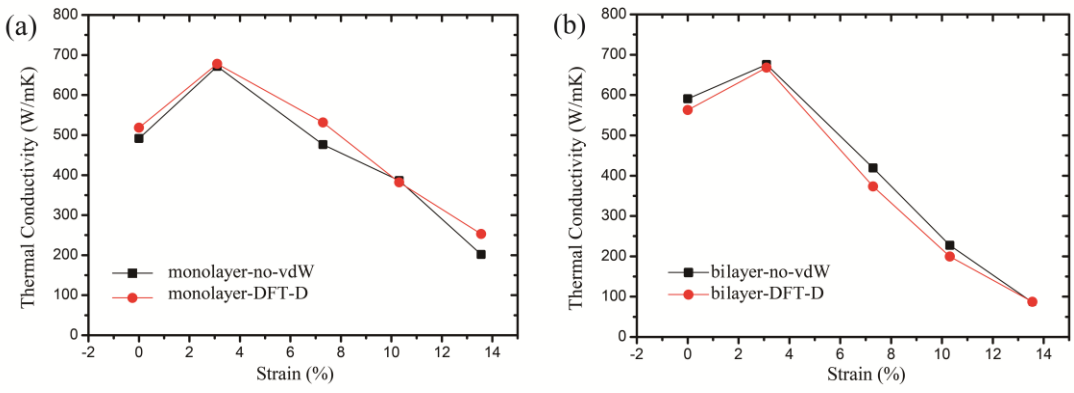

Fig. S2 The comparison of strain dependent thermal conductivity with infinite size at

room temperature when considering vdW interactions included (DFT-D) or not of (a) monolayer and (b) bilayer PG.

For a comparison, we also presented the calculation results not considering vdW functionals which are comparable to what considering vdW functionals, suggesting that the impact of vdW functionals on the thermal conductivity can be ignored for monolayer PG. At the same time, for bilayer PG, whether to choose a functional to consider the vdW interactions slightly affects the results of calculated thermal properties except phonon dispersion (Frequency of ZA2 at Γ) and rMFP. It can be found that considering the vdW results in a slight increment in the thermal conductivity of the monolayer PG and a slight reduction in the thermal conductivity of the bilayer PG. We further calculate the thermal conductivity of monolayer and bilayer PG as a function of tensile strain (Fig. S2(a) and (b)). Tensile strains ε generated by stretching the optimized lattice constant a_0 of unstrained structure in both in-plane directions can be calculated by $\varepsilon=(a/a_0-1)\times 100\%$, where a is the optimized lattice constant of strained structure. In Fig. S2, it is easy to find that considering the vdW functionals results in an increment/decrement in the thermal conductivity of the monolayer/bilayer PG under every strain, which indicates that vdW functionals have little effect on thermal conductivity of PG. Fig. S3 presented the effect of considering vdW functionals on phonon group velocity, three-phonon scattering phase space and phonon lifetime for monolayer and bilayer PG under no strain. For monolayer PG, vdW functional has little effect on harmonic and anharmonic phonon properties (three-phonon scattering phase space). However, from Fig. S3(e) we can find that even though phonon lifetime has no difference in the frequency region beyond 10 THz, a slight increment occurs in the low frequency region (<10 THz). Therefore, the slight upward movement of the phonon

lifetime in the low frequency region (Fig. S3(e)), that is, the decrease of phonon anharmonicity, will decrease the intrinsic phonon-phonon scattering and give rise to the slight increase of thermal conductivity when considering DFT-D for monolayer PG. The reason may lie in the strain attenuated interaction between the lone-pair electrons on C atoms and the bonding electrons from neighboring C atoms in PG, leading to the weakened phonon anharmonicity.[15]

For bilayer PG, vdW functional has non-neglectable effect on both harmonic (group velocity in Fig. S3(b)) and anharmonic (lifetime in Fig. S3(f)) phonon properties. In Fig. S3(b), by considering vdW interactions using the vdW-DF2, there is an obvious shrinkage in the frequency of optical phonon branches and a decrement of group velocity of acoustic phonon branches. For DFT-D, in Fig. S3(f), not only an increment (in the frequency of 0-40 THz) but also a decrement (in the frequency of 2-10 THz) of phonon lifetime happens in some phonon modes. For vdW-DF2, in Fig. S3(f), a slight increment of phonon lifetime occurs in the low frequency region (<10 THz) which is the same as DFT-D for monolayer PG. The vdW-DF2 has little effect on thermal conductivity because of the results of decrement of group velocity coupled with increment of phonon lifetime. Thus, the slight downward movement of the group velocity (Table S1 and Fig. S3(b)) and of phonon lifetime in part of frequency region (1-10 THz) plays an important role in the slight decrement of the lattice thermal conductivity when considering DFT-D for bilayer PG.

At present stage, we propose that the thermal conductivity of PG is not sensitive to DFT-D and vdW-DF2 vdW functionals. As a contrast, the thermal conductivity of graphene was reported to range from 1936 to 4376 W/mK and thermal properties have large difference with different XC functionals employed.[16] Thus, it can be concluded that the pentagonal structure like PG is completely different from graphene when it

comes to considering vdW functionals, which may lie in the buckled structure of PG.

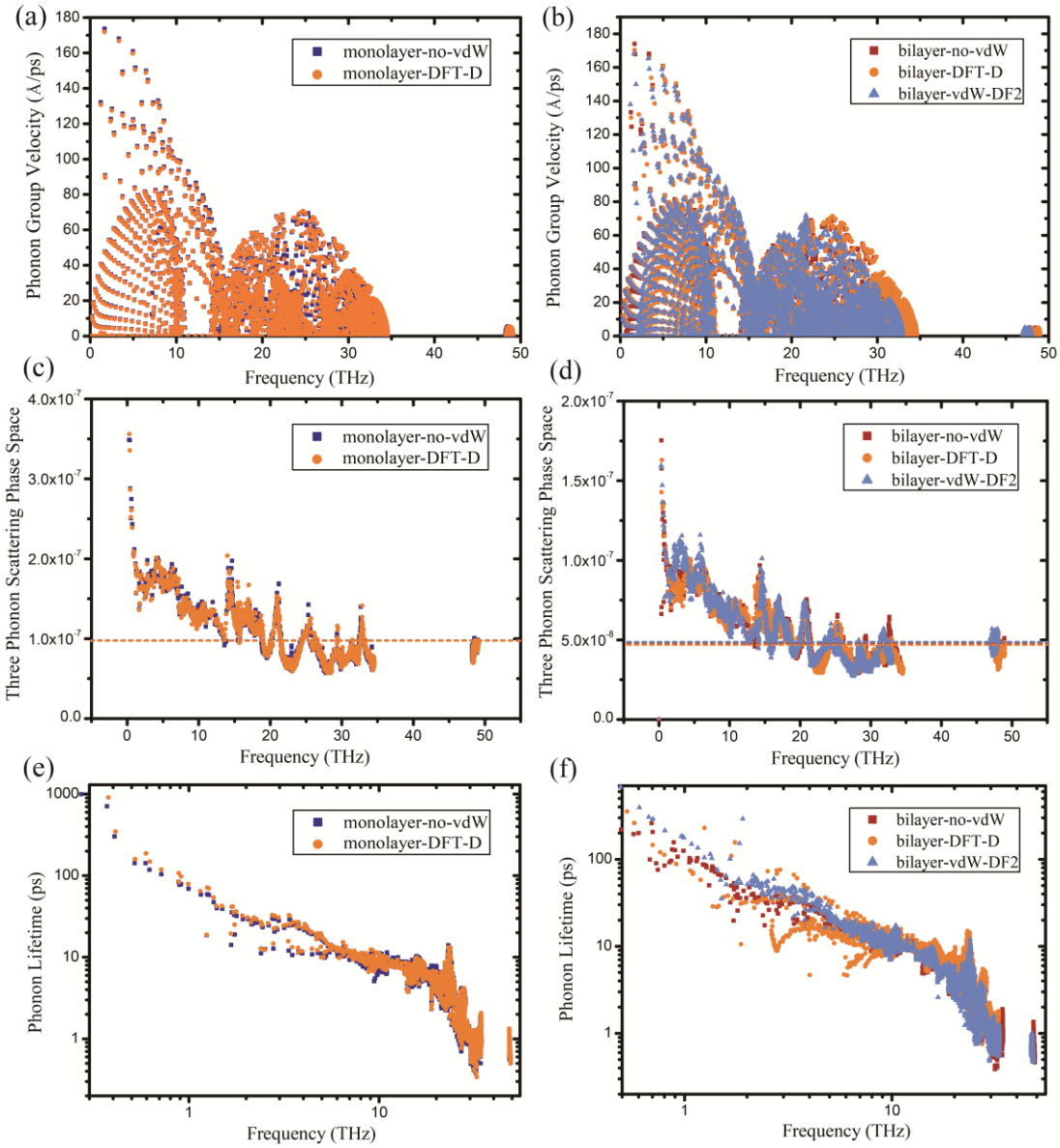

Fig. S3 Effect of vdW interactions on the mode level (a, b) phonon group velocity, (c, d) three-phonon scattering phase space and (e, f) phonon lifetime (from relaxation time approximation) for monolayer and bilayer PG, respectively. The dash lines in (c, d) mean the average value of phase space.

4. The considered range of strain.

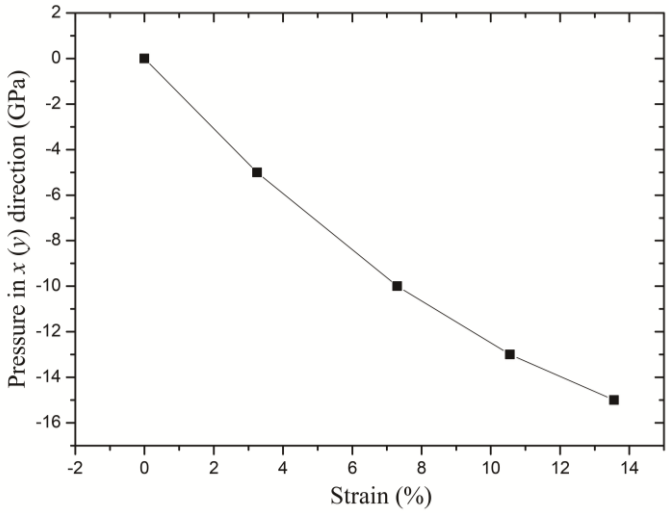

Fig. S4 Pressure in *x* (*y*) direction as a function of tensile strain.

5. The thermodynamic stability within considered range of strain

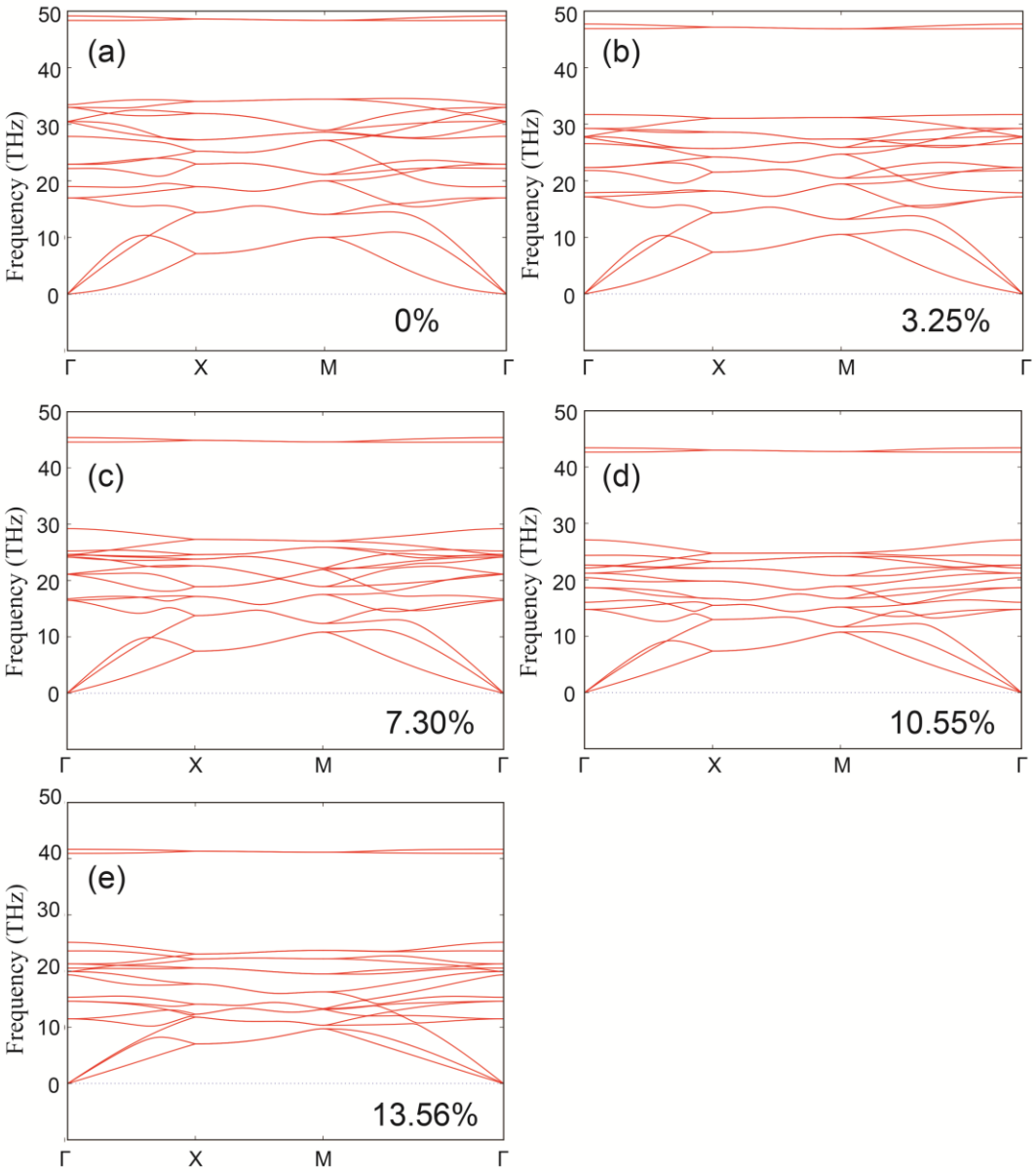

Fig. S5 Phonon dispersion curves of monolayer PG along the Γ−X−M−Γ at (a) 0%, (b) 3.25%, (c) 7.30%, (d) 10.55% and (e) 13.56% tensile strain.

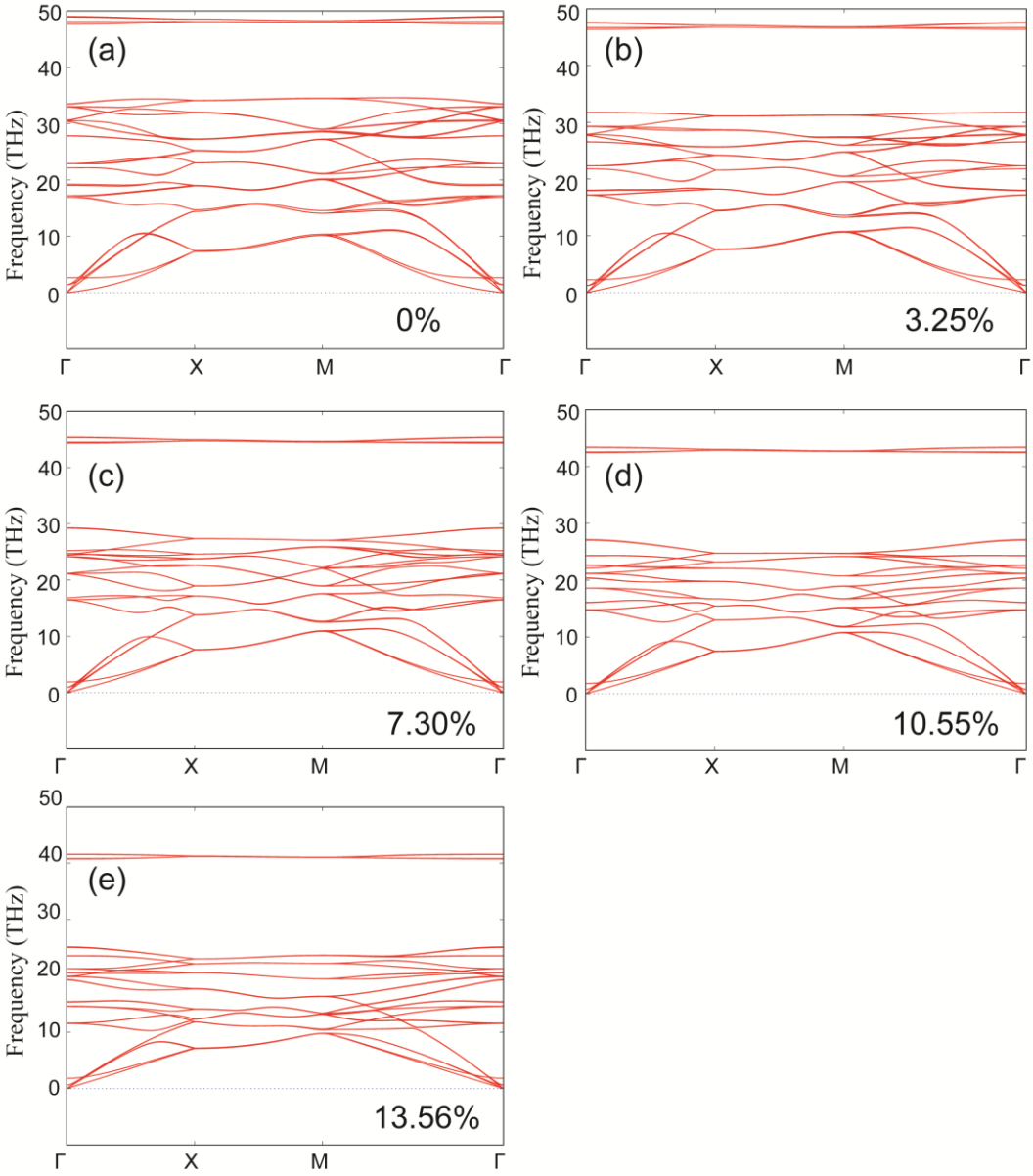

Fig. S6 Phonon dispersion curves of bilayer PG along the Γ−X−M−Γ at (a) 0%, (b) 3.25%, (c) 7.30%, (d) 10.55% and (e) 13.56% tensile strain.

6. The comparison of Grüneisen parameter between monolayer and bilayer PG

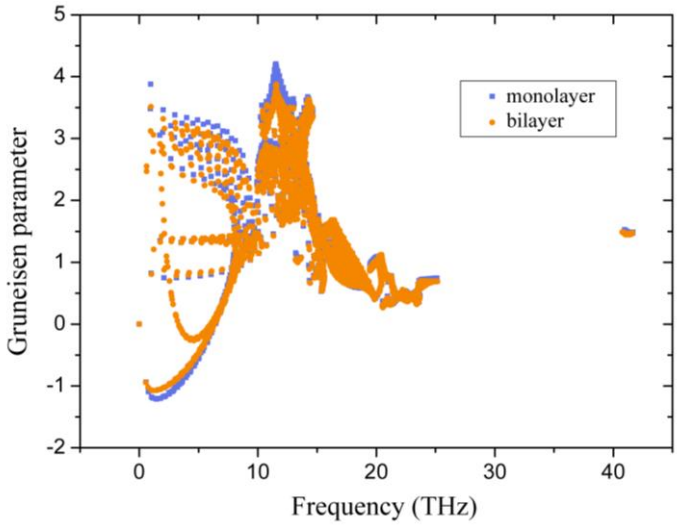

Fig. S7 A comparison on mode level of Grüneisen parameter between monolayer and bilayer PG at high tensile strain (13.56%).

References

1. G. Qin, Z. Qin, W.-Z. Fang, L.-C. Zhang, S.-Y. Yue, Q.-B. Yan, M. Hu and G. Su, *Nanoscale*, 2016, **8**, 11306-11319.
2. W. Li, J. Carrete, N. A. Katcho and N. Mingo, *Comput. Phys. Commun.*, 2014, **185**, 1747-1758.
3. M. Omini and A. Sparavigna, *Physica B*, 1995, **212**, 101-112.
4. L. Lindsay and D. Broido, *J. Phys. Condens. Mat.*, 2008, **20**, 165209.
5. A. Ward, D. Broido, D. A. Stewart and G. Deinzer, *Phys. Rev. B*, 2009, **80**, 125203.
6. A. Ward and D. Broido, *Phys. Rev. B*, 2010, **81**, 085205.
7. M. Omini and A. Sparavigna, *Phys. Rev. B*, 1996, **53**, 9064.
8. A. Kundu, N. Mingo, D. Broido and D. Stewart, *Phys. Rev. B*, 2011, **84**, 125426.
9. G. Stefan, E. Stephan and G. Lars, *J. Comput. Chem.*, 2011, **32**, 1456-1465.
10. G. Stefan, A. Jens, E. Stephan and K. Helge, *J. Chem. Phys.*, 2010, **132**, 154104.
11. T. Thonhauser, S. Zuluaga, C. A. Arter, K. Berland, E. Schröder and P. Hyldgaard, *Phys. Rev. Lett.*, 2015, **115**, 136402.
12. K. Lee, É. D. Murray, L. Kong, B. I. Lundqvist and D. C. Langreth, *Phys. Rev. B* 2010, **82**, 081101.
13. K. Berland, V. R. Cooper, K. Lee, E. Schröder, T. Thonhauser, P. Hyldgaard and B. I. Lundqvist, *Rep. Prog. Phys.*, 2015, **78**, 066501.
14. D. C. Langreth, B. I. Lundqvist, S. D. Chakarovaäck, V. R. Cooper, M. Dion, P. Hyldgaard, A. Kelkkanen, J. Kleis, L. Kong and S. Li, *J. Phys. Condens. Mat.*, 2009, **21**, 084203.
15. G. Qin, Z. Qin, H. Wang and H. Ming, *Nano Energy*, 2018, **50**, 425-430.
16. G. Qin, Z. Qin, H. Wang and M. Hu, *Comput. Mater. Sci.*, 2018, **151**, 153-159.